



HAL
open science

Modeling approaches to assimilating L band passive microwave observations over land surfaces

Jean-Pierre Wigneron, André Chanzy, Jean-Christophe Calvet, Albert Oliso, Yann H. Kerr

► **To cite this version:**

Jean-Pierre Wigneron, André Chanzy, Jean-Christophe Calvet, Albert Oliso, Yann H. Kerr. Modeling approaches to assimilating L band passive microwave observations over land surfaces. *Journal of Geophysical Research*, 2002, 107 (D14), pp.1-14. 10.1029/2001JD000958 . hal-02682121

HAL Id: hal-02682121

<https://hal.inrae.fr/hal-02682121>

Submitted on 11 Jan 2021

HAL is a multi-disciplinary open access archive for the deposit and dissemination of scientific research documents, whether they are published or not. The documents may come from teaching and research institutions in France or abroad, or from public or private research centers.

L'archive ouverte pluridisciplinaire **HAL**, est destinée au dépôt et à la diffusion de documents scientifiques de niveau recherche, publiés ou non, émanant des établissements d'enseignement et de recherche français ou étrangers, des laboratoires publics ou privés.

Modeling approaches to assimilating *L* band passive microwave observations over land surfaces

Jean-Pierre Wigneron,¹ André Chanzy,² Jean-Christophe Calvet,³ Albert Olioso,² and Yann Kerr⁴

Received 19 June 2001; revised 16 November 2001; accepted 27 November 2001; published 31 July 2002.

[1] *L* band passive microwave remotely sensed data have great potential for providing estimates of soil moisture with high temporal sampling and on a regional scale. Several studies have shown the possibility of assessing the hydrological conditions deep down in soil (in the top 1 or 2 m) from these repetitive estimates of surface soil moisture. Water availability for plants, which is related to soil moisture in the root zone, is a key variable for estimating the evapotranspiration fluxes over land surfaces. This estimation is an important issue for meteorological and hydrological modeling, since it is a basic term of land surface forcing in mesoscale atmospheric circulations. However, at the present time the assimilation approach of remotely sensed brightness temperature data for operational use in the fields of meteorology and hydrology is poorly defined and important issues remain to be addressed in order to develop an operational assimilation approach. Two important issues are to identify (1) how vegetation variables describing vegetation development can be accounted for and (2) how the attenuation effects of *L* band microwave radiation within the canopy layer can be computed on large spatial scales. On the basis of an exhaustive data set including multiangular and dual-polarization passive microwave measurements acquired over a wheat crop during a 3-month period in 1993, two main modeling approaches are tested in this study. The principle of both approaches was based on the use of dual-polarization and multiangular observations to discriminate between the effects of soil and vegetation on the crop microwave signature. For the two approaches, both the initial soil water reservoir R_2 (at the beginning of the crop development) and parameterizations of the crop development could be retrieved simultaneously from the assimilation of the passive microwave measurements. From these results, promising assimilation strategies can be expected from the multiangular Soil Moisture and Ocean Salinity (SMOS) observations made over the land surface. **INDEX TERMS:** 1640 Global Change: Remote sensing; 1818 Hydrology: Evapotranspiration; 1866 Hydrology: Soil moisture; 3322 Meteorology and Atmospheric Dynamics: Land/atmosphere interactions; 3360 Meteorology and Atmospheric Dynamics: Remote sensing; **KEYWORDS:** Microwave radiometry, soil moisture, vegetation biomass, global change, assimilation, coupling radiative transfer and soil-vegetation-atmosphere-transfer (SVAT) models

1. Introduction

[2] Soil moisture is highly variable both spatially and temporally in the natural environment as a result of inhomogeneity of soil properties, topography, land cover, and the nonuniformity of rainfall and evapotranspiration. Remotely sensed data, which can provide frequent and spatially comprehensive estimates of land surface characteristics, arouse great interest. *L* band passive microwave

remote sensing sensors are able to provide estimates of surface soil moisture, on both spatial and temporal scales, compatible with applications in the fields of meteorology and hydrology [Schmugge *et al.*, 1974; Schmugge and Jackson, 1994; Njoku and Entekhabi, 1996; Jackson *et al.*, 1999]. An *L* band passive mission (the Soil Moisture and Ocean Salinity mission (SMOS) [Kerr *et al.*, 1999]) was recently selected as a “minisatellite mission” by the Centre National d’Etudes Spatiales (CNES, France) and then for phase A studies by the European Space Agency (ESA) as the second Earth Explorer Opportunity Mission. The SMOS payload is an *L* band radiometer based on an innovative two-dimensional aperture synthesis concept. This sensor has new and significant capabilities, especially in terms of multiangular viewing configurations. The potential of this radiometer for monitoring surface variables over land surfaces was analyzed by Wigneron *et al.* [2000]. From the results of this study, promising retrieval capabilities of both soil moisture and vegetation optical depth (which accounts

¹Institut National de la Recherche Agronomique, Unité de Bioclimatologie, Villenave d’Ornon, France.

²Institut National de la Recherche Agronomique, Climat, Sol et Environnement, Agroparc, Avignon, France.

³Météo France/Centre National de Recherche de la Meteorologie, Toulouse, France.

⁴Centre National d’Etudes Spatiales/Centre d’Etude Spatial de la Biosphere, Toulouse, France.

for the attenuation effects of microwave radiation within the canopy layer) can be expected from SMOS over the land surface.

[3] Surface soil moisture (hereafter referred to as w_S) is a key variable of water and energy exchanges at the land surface/atmosphere interface. This variable is of crucial importance for several reasons: in hydrology and meteorology, the water content of the surface soil layer is a pertinent descriptor of water exchanges between the surface and the atmosphere [Chanzy and Bruckler, 1993; Daamen and Simmonds, 1996]. Also, soil moisture is an important variable for estimating the distribution of precipitation between storm runoff and storage and for computing several key variables of land surface energy and water budget (albedo, hydraulic conductivity, etc.). L band microwave remote sensing measurements are sensitive to the average moisture content of a surface layer corresponding roughly to the 0–5 cm topsoil layer. Therefore this technique cannot provide direct estimates of water availability for plants that is related to the soil moisture in the root zone (hereafter referred to as w_2) and root depth. Water availability for plants is a key variable for estimating the evapotranspiration fluxes (ET) over land surfaces. This estimation is thus an important issue for meteorological modeling, since it is a basic term of land surface forcing in mesoscale atmospheric circulations [Noilhan and Calvet, 1995].

[4] Several studies have shown that modeling the heat and mass flow within soil can be used to derive information about the soil water content at depth from temporal surface soil moisture information. The feasibility of using brightness temperature measurements (microwave and infrared channels) to solve the inverse problem associated with soil moisture and heat profile was demonstrated by Entekhabi *et al.* [1994] over bare soils. This theoretical analysis was based on a Kalman filter using radiative transfer and coupled moisture and heat diffusion equations. Burke *et al.* [1997] retrieved soil hydraulic properties by calibrating a coupled model from time series of microwave brightness temperatures over agricultural fields. Retrievals of root zone soil moisture were carried out by Calvet *et al.* [1998a] during the Murex experiment [Calvet *et al.*, 1999]. The study is based on a continuous series of micrometeorological data measured in southwestern France on a fallow site in 1995–1996. A meteorological surface scheme (ISBA) [Noilhan and Planton, 1989], including the force-restore modeling of water and heat transfers in soil, was used to retrieve variables at depth from the ground measurements of w_S . It was found that one measurement of w_S every 3–4 days during a minimal 15-day period was sufficient to obtain accurate estimates of w_2 . On the basis of the same assimilation approach, Wigneron *et al.* [1999a] investigated the accuracy of the soil reservoir retrievals as a function of the time period and frequency of measurements of surface soil moisture involved in the retrieval process. Sequential and variational data assimilation approaches have been tested, respectively, with experimental bare soil data sets [Galan-towicz *et al.*, 1999] and with a series of synthetic experiments based on the Southern Great Plains 1997 Hydrology experiments [Reichle *et al.*, 2001]. These studies showed the possibility of assessing the hydrological conditions deep down in soil (in the top 1 or 2 m) from repetitive estimates of water content at the soil surface.

[5] For applications in meteorology and hydrology, a spatial resolution of 20–50 km would be required (a pixel size larger than 50 km would be too large for mesoscale models). Also, a revisit time of one or 2-day was required in hydrology to track quick drying periods after rainfalls. In meteorology, retrievals of root zone soil moisture should be carried out with a 3- to 5-day time frequency for short- to medium-term meteorological modeling [Kerr *et al.*, 1999]. However, at the present time the modeling approach to assimilating remotely sensed brightness temperature data for operational use in meteorology and hydrology is poorly defined. No microwave radiometric measurements were available in the study of Calvet *et al.* [1998a] and Wigneron *et al.* [1999a], and the retrievals of root zone soil moisture were based on times series of ground measurements of surface soil moisture w_S . Thus, in the two above studies it was not possible to fully investigate model uncertainties. Specifically, the errors due to the radiative transfer model used to simulate the canopy microwave emission could not be analyzed. More generally, in the literature, very few studies have investigated which modeling approach would be best suited for taking into account vegetation effects in the assimilation scheme of the passive L band brightness temperature (T_B). Concerning these aspects, two key questions must be addressed for developing an operational assimilation approach of the T_B data. These two questions are the following:

1. How can we account for vegetation variables (leaf area index (LAI), biomass, etc.), which describe vegetation development? These variables are important inputs to the soil-vegetation-atmosphere-transfer (SVAT) models used in the assimilation process. For instance, in most previous studies, leaf area index (LAI), which is prescribed to the SVAT model is generally obtained from ground-based measurements. Several research groups (National Aeronautics and Space Administration (NASA) and National Oceanic and Atmospheric Administration (NOAA)) are working to generate LAI products routinely from optical remote sensing observations. These products could be used as ancillary LAI estimates, for accounting for vegetation growth in the assimilation scheme of spaceborne passive microwave remote sensing observations. However, it is likely that this process limit the operational use of the passive microwave observations for monitoring land surfaces in all weather conditions.

2. How can we account for vegetation optical depth (τ), which is used to parameterize the attenuation effects of microwave radiation within the canopy layer? This parameter is generally derived from the product of vegetation water content (W_C , kg/m²) and a parameter b ($b \approx 0.12 +/ - 0.3$), which depends on vegetation type, polarization, and view angle [Jackson and Schmugge, 1991]. However, for an operational use of the assimilation approach, estimating these two parameters on large spatial scales from ancillary remotely sensed data is not an easy task.

[6] The present study investigates these two important issues. Two modeling approaches to monitoring both vegetation and soil characteristics from the assimilation of time series of passive microwave data are tested. Contrary to the above mentioned studies by Calvet *et al.* [1998a] and Wigneron *et al.* [1999a], the present analysis is based on a data set including passive microwave measurements

acquired over a wheat crop during a 3-month period in 1993. The measurements were acquired by the multifrequency PORTOS radiometer (the experiment will be referred to as the PORTOS-93 experiment). Dual-polarization and multiangular observations were made in the 0° – 50° range, corresponding to the instrument capabilities of the SMOS mission. The data set also included measurements of flux data (latent and sensible heat flux, soil conduction, etc.), and soil and vegetation characteristics. The multiangular T_B data were assimilated in a synthetic model coupling a simple radiative transfer model, simulating the brightness temperature (“TB model”) of the wheat canopy, to a SVAT model (ISBA), simulating the energy and mass exchanges at the soil-vegetation-atmosphere interface. Two different assimilation schemes were tested and compared in this study. Assimilation of times series of T_B in the coupled SVAT/TB model (SVAT/TB) was carried out and two modeling approaches toward accounting for vegetation effects were implemented and tested:

Approach I: the variable τ is retrieved from the assimilation process concurrently with the soil water reservoir R_2 . This idea of developing such an approach directly resulted from studies by *Wigneron et al.* [1995, 2000] showing that it is possible to retrieve simultaneously information on soil and vegetation (namely soil moisture and vegetation optical depth) from dual-polarization and multiangular L band passive microwave measurements. Note that the two studies showed that the information content of monopolarization and/or monoangular observations was probably not sufficient to perform this simultaneous retrieval process. As the PORTOS-93 data set included dual-polarization and multiangular observations, the possibility to retrieve simultaneously information on soil and vegetation (namely root zone soil moisture R_2 and vegetation optical depth) from the assimilation process could be tested in this study.

Approach II: a fully integrated assimilation approach is implemented: interactive vegetation SVAT model (ISBA-Ags) is used to simulate all the inputs of the TB model (namely surface soil moisture, surface temperature and optical depth). In this latter approach, no ancillary data describing vegetation development or time variations in optical depth are required (all this information can be directly derived from the ISBA-Ags simulations). As for approach I, approach II is based on the principle that it is possible to retrieve information on both soil and vegetation from the assimilation of dual-polarization and multiangular observations.

[7] The results of this study demonstrate the potential of multiangular passive microwave measurements as measured by the SMOS instrument for monitoring both vegetation and soil variables through assimilation in an interactive vegetation SVAT model.

2. Material

2.1. Data Set

[8] The passive microwave measurements were acquired during the whole growth cycle of a wheat crop (*Triticum durum*, cultivar prinqual) in spring 1993, from 19 April (DoY 109) to 7 July (DoY 188) just before harvest. The sowing date (19 March = DoY 78) was late and the crop cycle was rather short. Multifrequency (1.4,

5, 10.6, 23.8, 36.5, and 90 GHz) and dual-polarization (at H and V polarization) measurements were acquired by the PORTOS radiometer, but only L band measurements (at 1.4 GHz) were considered in this study. PORTOS was designed by the French National Space Agency (CNES) and built by Astrium in 1990/1991. During the experiment it was mounted on a 20-m crane boom, and the measurements were made at different view angles θ (from $\theta = 0^\circ$ to $\theta = 50^\circ$ or 60°). In this study, the look direction of the radiometer was parallel to the row direction of the wheat field. Absolute calibrations were performed regularly during the experiment, over calm water surfaces and eccosorb slabs. After calibration, the absolute and relative accuracy of the radiometer measurements was ~ 5 K and 2–3 K, respectively (in terms of brightness temperature) at 1.4 GHz. The rather low absolute sensor accuracy value was mainly due to difficulties in correcting for the effects of the 1.4-GHz antenna losses and of the antenna sidelobes on the measured surface emission. The radiometric relative accuracy of ~ 2 – 3 K corresponds to relative errors of ~ 0.01 m^3/m^3 in terms of soil moisture estimates over bare soil surfaces [*Ulaby et al.*, 1986]. This is to be noted, since the 0.04 m^3/m^3 threshold is considered as the required accuracy for studies over land surfaces in hydrology and meteorology [*Kerr et al.*, 1999]. Therefore the PORTOS radiometric errors at L band can be considered as sufficiently low to enable assimilation studies. Over the DoY 109 to DoY 188 period, there were 45 microwave measurement dates, which corresponds to a time frequency of about four measurement dates each week. The microwave observations used in this study were acquired at different hour of day (at morning, afternoon, or evening). The microwave observations are illustrated in Figure 1 at a view angle $\theta = 0^\circ$ and at H polarization. Rapid changes in the value of T_B (for instance on DoY 119, 133, and at the end of the crop cycle) were related to rapid changes in the surface soil moisture w_S , due to rainfall or irrigation. Conversely the trend of T_B (which was obtained in Figure 1 by “smoothing” the T_B observations using a standard sliding window filtering technique), i.e., the increase in T_B from DoY 118 to about DoY 160, and then the decrease up to DoY 180, was related to the crop cycle: growth and then senescence of the wheat canopy. Therefore the L band microwave observations were highly sensitive to time variations in both vegetation and soil characteristics. Note that the crop average surface temperature continuously increased during the whole radiometric measurement period. Therefore the trend of T_B in Figure 1 cannot be explained by changes in the surface temperature.

[9] For each date of microwave measurements a detailed characterization of the soil moisture profile was carried out, from gravimetric measurements in the upper 0–10 cm soil layer (0–1, 1–2, 2–3, 3–5, 5–10 cm soil layers were sampled) and from neutron probes in the 10–150 cm soil layer at 10-cm intervals. Vegetation characteristics (crop height (H_C), leaf area index (LAI), amount of water in the canopy (W_C), moisture content of leaves and stems (percent)) were measured twice a week during crop growth. To illustrate the time variations in the vegetation characteristics during the crop cycle, the time variations in W_C , LAI, and H_C are given in Figure 2. The value of W_C shown in Figure 2 was obtained using a parametric “growth curve”

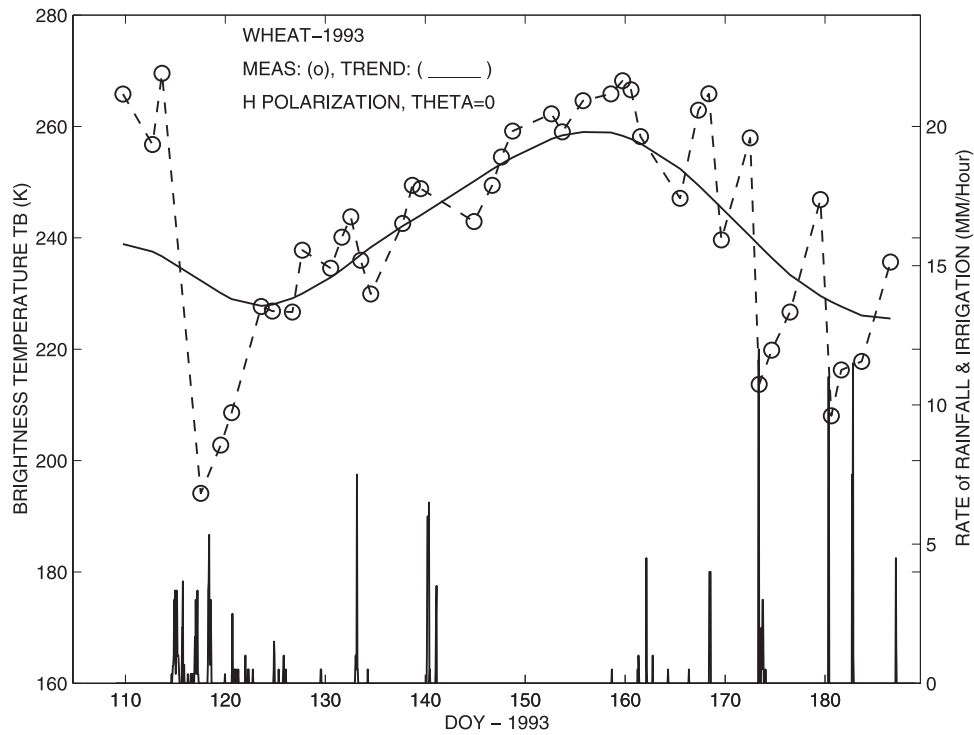


Figure 1. Microwave observations over the wheat field at view angle $\theta = 0^\circ$, at H polarization (open circles). The trend (solid lines) was obtained using a standard sliding window filtering technique. Rain and irrigation rates (mm h^{-1}) are indicated by vertical solid lines.

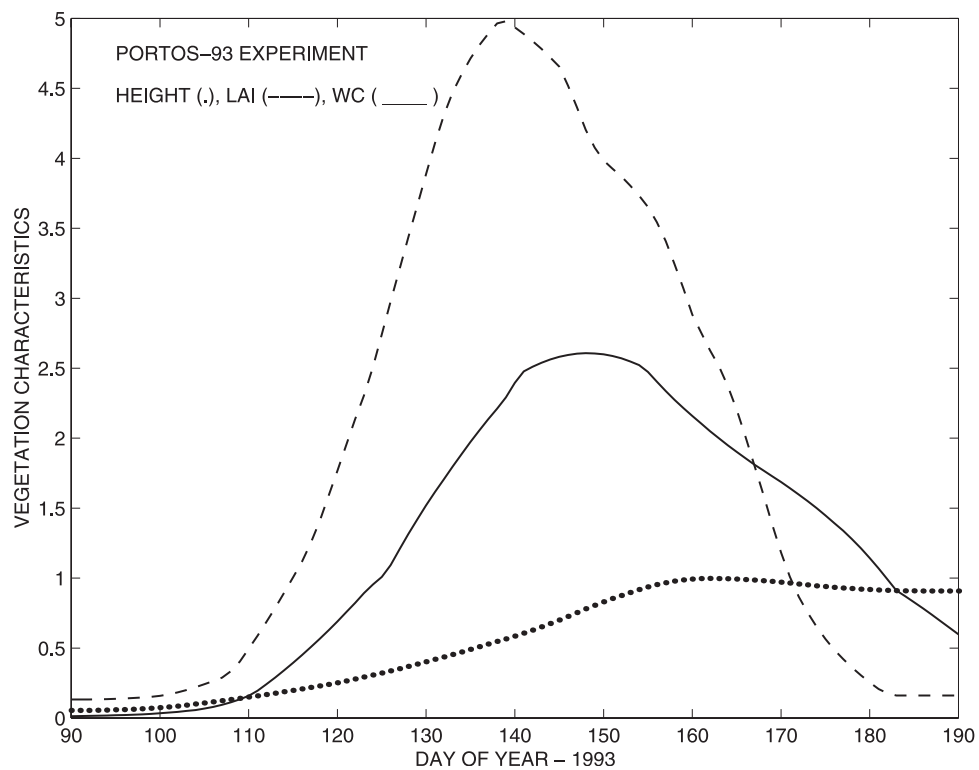


Figure 2. Time variations in wheat characteristics during the crop cycle: vegetation water content W_C (kg/m^2) (solid lines), leaf area index (LAI) (dashed lines), and crop height H_C (dots).

Table 1. Soil and Vegetation Parameters of the Brightness Temperature (TB) Model^a

Characteristic	Value
<i>Wheat</i>	
Single scattering albedo ω	$\omega(1.4 \text{ GHz}) = 0.0$
Polarization correction factor	$\text{cpol} = 2.6$
<i>Soil (Silty Clay Loam)</i>	
Soil texture	
Clay C, %	$C = 27\%$
Sand S, %	$S = 11\%$
Dry bulk density ρ_d , g/cm ³	$\rho_d = 1.4$
Effective roughness parameters	$h_{\text{SOIL}} = 0.2, N_{\text{SOIL}} = 0$

^aFrom Wigneron et al. [1995, 2000].

[Wigneron et al., 1999b] calibrated from ground-based measurements of W_C :

$$W_C(t) = K \left\{ \frac{1}{1 + \exp[-a(t - T_I)]} - \frac{1}{1 + \exp(-b(t - T_S))} \right\}, \quad (1)$$

where t is time (day), with $K = 4.251$, $a = 0.1176$, $T_I = 131.20$, $b = 0.0636$, $T_S = 163.667$.

[10] Note that at the end of the crop cycle, several intensive irrigations were carried out over the senescent wheat canopy. During irrigation, stems and ears bent, due to the increasing weight of the water intercepted by the vegetation canopy. The structure of the canopy was greatly modified by these irrigation events.

[11] Detailed measurements of the mass and energy transfers at the soil-vegetation-atmosphere interface (net radiation (R_N), latent (L_E) and sensible (H) heat flux, soil conduction (G) and standard meteorological observations at 2-m height were acquired on a 15-min basis during the whole crop cycle. Several modeling and retrieval studies over vegetation and bare soils have been based on this data set. In particular, more information concerning measurements over the wheat field can be found in the works of Wigneron et al. [1995, 1996].

2.2. TB Model

[12] The TB model is a simple zeroth-order radiative transfer model used in retrieval studies based on the PORTOS-93 data set [Wigneron et al., 1995, 2000]. Brightness temperature (T_B) depends on both soil and vegetation characteristics. The microwave emission of soil is highly dependent on surface soil moisture w_S (roughly in the upper 3-cm soil layer) and, to a lesser extent, on soil roughness and temperature. The vegetation canopy attenuates soil emission (this effect is parameterized by the vegetation optical depth τ) and adds its own emission to the total canopy emission. The ‘‘TB model,’’ which is used to simulate microwave brightness temperature T_B , accounts for both these soil and vegetation effects. In this model, two main parameters account for the effects of vegetation: optical depth (τ) and the single scattering albedo (ω), which parameterizes scattering effects. Usually, an estimate of optical depth (referred to as τ_W in this study) can be obtained from the amount of water in the canopy (W_C) using the simplified relationship:

$$\tau_W = bW_C, \quad (2)$$

where b is a parameter depending on the vegetation type.

[13] A detailed description of the TB model can be found in the works of Wigneron et al. [1995, 2000]. The input

parameters of the TB model were obtained from ground based measurements or calibrated by Wigneron et al. [1995]. These parameters are given in Table 1. The main input variables of this model are surface temperature (T_S) and surface soil moisture (w_S), which are both simulated by the ISBA model, and optical depth (τ). The surface soil moisture (w_S) used in this study was computed over the upper 0–3 cm soil layer, which corresponds roughly to the effective layer contributing to soil microwave emission [Raju et al., 1995].

3. Methods

[14] In the assimilation process, brightness temperature measurements are used to constrain the SVAT model, which simulates the surface variables of interest. Brightness temperatures are assimilated in a synthetic model, coupling a radiative transfer model (the TB model) simulating brightness temperature T_B , to a SVAT model simulating energy and mass exchanges at the soil-vegetation-atmosphere interface. In this study our objective was not to compare different assimilation schemes from a quantitative analysis of the results. The PORTOS-93 data set used in this study included monitoring only one vegetation type during a rather short period of time (~ 3 months) and for specific climatic conditions. This data set is not sufficient for developing a quantitative comparison or calibration/validation approach. Long-term experimental campaigns during a 2- or 3-year time period over several vegetation canopies, such as that scheduled in Toulouse by Météo-France [Calvet et al., 2001], would be required for this comparison. The main objective of this study was to provide some new insights into the possibility of implementing assimilation schemes of T_B data that could be compatible with an operational use in the fields of meteorology and hydrology. To this end, assimilation methods based on two different modeling schemes were tested in this work.

3.1. Approach I: Assimilation in the (ISBA/TB) Model

[15] The general principle of the coupling for approach I is given in Figure 3. The SVAT model is the Interactions between Soil-Biosphere-Atmosphere (ISBA) model, which was used in the previous assimilation studies by Calvet et al. [1998a] and Wigneron et al. [1999a]. The ISBA land surface scheme was developed by Météo-France and is used in the operational simulations of the French weather forecast model. The main surface variables simulated by ISBA considered in this study are surface temperature T_S , surface soil moisture w_S (m^3/m^3), soil water reservoir R_2 (mm), which can be directly related to mean soil moisture w_2 (m^3/m^3) and root depth d_2 (m) ($R_2 = 1000 w_2 d_2$), water content of an interception reservoir (W_r) and flux data (R_N , L_E , H , and G). The ISBA model is driven by measurements of atmospheric forcing variables on a 30-min basis. Two vegetation characteristics (LAI and crop height H_C), obtained from ground-based measurements, were ascribed on a daily basis. The ISBA input parameters (which are considered to remain constant during the crop cycle) are given in Table 2. These parameters were calibrated on the same test site by Wigneron et al. [1999a] over a soybean crop. Only one parameter (minimum stomatal resistance $r_{S\text{min}}$) was modified and set at 80 s/m, which is a typical value for Mediterranean crops [Habets, 1998].

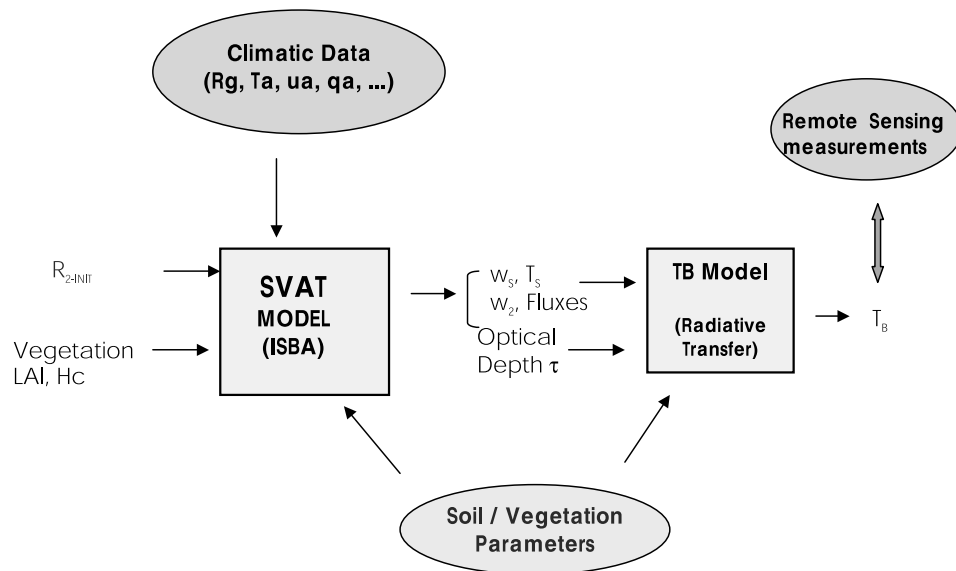


Figure 3. General principle of the coupling between Interactions between Soil-Biosphere-Atmosphere (ISBA) and the brightness temperature (TB) model (approach I). The variables to be retrieved from the T_B measurements were initial soil water content (R_{2-INIT}) and time variations in optical depth τ .

[16] This simple coupled model ISBA/TB was used in approach I. In this approach, both initial soil water reservoir R_2 at date $t = \text{DoY } 109$ (R_{2-INIT}) and time variations in optical depth τ were retrieved from the assimilation process of the T_B data. The assimilation approach was similar to that of previous studies by *Calvet et al.* [1998a], except that our analysis was based on T_B data and not on ground-based measurements of surface soil moisture w_s . Retrievals of both R_{2-INIT} and $\tau(t)$ were carried out using a simple assimilation process consisting of minimizing the root mean square (rms) error between measured and simulated brightness temperatures during the assimilation period. To obtain an accurate description of time variations in τ during the whole vegetation development period, the assimilation of T_B was carried out during an 80-day period (from DoY 109

to DoY 188). This assimilation period included the T_B measurements made over the senescent canopy. The computation of the rms error was carried out for both polarizations (vertical and horizontal) and for five incidence angles θ ($\theta = 0^\circ, 10^\circ, 20^\circ, 30^\circ, \text{ and } 40^\circ$). This computation included all the brightness temperature measurements available during the (DoY 109 to DoY 188) assimilation period (about four measurement dates were available every week). Since optical depth is usually related to total crop water content (W_C), it was assumed in this study that time variations in τ can be well approximated by the same parametric “growth curve” as that given for W_C in equation (1). Therefore, by assimilation of the T_B data, six parameters were retrieved in approach I: R_{2-INIT} and the five parameters (K, a, T_b, b, T_s) describing time variations in τ .

Table 2. Soil and Vegetation Parameters for the ISBA and ISBA-Ags Model

Definition	Symbol and Value	Source
<i>Soil</i>		
Texture		<i>Wigneron et al.</i> [1999a]
Sand fraction, %	sand = 11	
Clay fraction, %	clay = 27	
Soil depth, m	$d_2 = 1.5$	measured
Wilting point, m^3/m^3	$w_{WILT}^M = 0.18$	<i>Wigneron et al.</i> [1999a]
Field capacity, m^3/m^3	$w_{FC}^M = 0.31$	<i>Wigneron et al.</i> [1999a]
Water transfer coefficient	$C_1/d_1 = 300$	<i>Wigneron et al.</i> [1999a]
<i>Vegetation</i>		
Vegetation coverage	veg = $1 - \exp(-0.6 \cdot \text{LAI})$ veg ≤ 0.8	<i>Habets</i> [1998]
Albedo	$A = 0.22$	<i>Wigneron et al.</i> [1999a]
Thermal emissivity	$\epsilon_s = 0.97$	<i>Wigneron et al.</i> [1999a]
Roughness length, m	$z_0 = 0.13 H_c$ ($H_c = \text{crop height}$)	<i>Wigneron et al.</i> [1999a]
Roughness length ratio	$z_0/z_{0h} = 10$	<i>Wigneron et al.</i> [1999a]
Displacement height, m	$d = 0.7 \cdot H_c$ ($H_c = \text{crop height}$)	<i>Wigneron et al.</i> [1999a]
Specific to ISBA (approach I)		
Minimum stomatal resistance	$r_{smin} = 80 \text{ sm}^{-1}$	<i>Habets</i> [1998]
Specific to ISBA-Ags (approach II)		
Mesophyll conductance	$g_m = 7 \text{ mm/s}$	<i>Voirin</i> [1999]
Leaf life expectancy	$D_E = 50 \text{ day}$	<i>Voirin</i> [1999]
Ratio: LAI/crop height, m	$\text{LAI}/H_C = 6$	measured

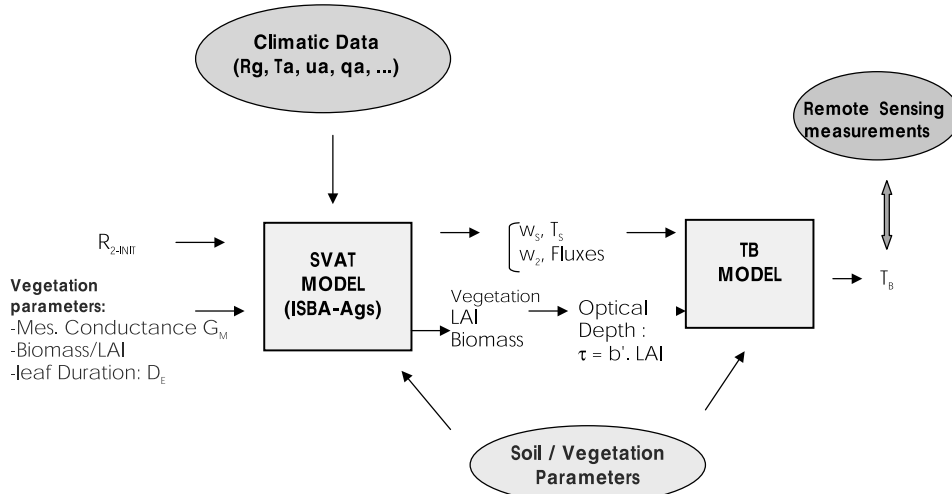


Figure 4. General principle of the coupling between ISBA-Ags and the TB model (approach II). The parameters to be retrieved from the T_B measurements were initial soil water content (R_{2-INIT}) and the vegetation parameter (B/LAI).

3.2. Approach II: Assimilation in the (ISBA-AGS/TB) Model

[17] In approach II a new version of the ISBA model (“the ISBA-Ags” model) was used [Calvet *et al.*, 1998b]. In this new version the physiological stomatal resistance scheme proposed by Jacobs *et al.* [1994] was used to describe photosynthesis and its coupling with stomatal resistance at the leaf level. In addition, plant response to soil water stress was driven by a normalized soil moisture factor applied to the mesophyll conductance (g_M). The computed net vegetation assimilation can be used to feed a simple growth submodel and to predict the density of the vegetation cover. Three main parameters are needed to calibrate ISBA-Ags: leaf life expectancy (D_E) and effective biomass per unit leaf area (B/LAI) to calibrate the growth submodel, and mesophyll conductance (g_M). Once calibrated, the ISBA-Ags model is able to simulate water budget, fluxes (CO_2 , sensible and latent heat fluxes, etc.) and LAI. Thus the model is able to adapt the simulations of vegetation growth in response to changes in the environmental conditions (precipitation distribution, soil moisture in the root-zone, climatic conditions, etc.) and, in contrast to ISBA, ISBA-Ags can be considered as “an interactive vegetation SVAT model.”

[18] The general principle of the coupling with ISBA-Ags in approach II is given in Figure 4. The main differences between this approach (Figure 4) and approach I (Figure 3) are the following:

1. The two vegetation characteristics (LAI and crop height H_C) were not obtained from ground-based measurements as in approach I. They were directly obtained from the ISBA-Ags simulations. LAI is an output of ISBA-Ags (this ISBA-Ags output will be referred to as LAI*). Crop height (H_C) is simply obtained by considering that

$$H_C = 6 \cdot LAI \quad (\text{approximate relationship derived for wheat crops}) \quad (3)$$

2. Optical depth (τ) was directly derived from the ISBA-Ags simulations. Using an approach similar to equation (2), it is assumed in this study that τ is proportional to LAI* according to:

$$\tau = b' LAI^*, \quad (4)$$

where b' is a parameter which depends mainly on the crop type and should be calibrated prior to the assimilation procedure.

[19] Note that after analyzing several vegetation data sets, we found that there is no general relationship between LAI and optical depth (or vegetation water content W_C) over crops (the ratio LAI/W_C depends on vegetation type, growth stage but also on climatic conditions (hydraulic stress, strong wind)). However, equation (4) is a simple and robust approximate formulation which may be considered as valid during most of the crop cycle (excluding early growth stages and the senescence period).

[20] The leaf area index (LAI*), which is simulated by ISBA-Ags, is representative of the whole metabolic biomass which contributes to photosynthesis and plant transpiration. Therefore LAI* may differ slightly from LAI values obtained from ground-based measurements which account only for green leaf area (for a well-developed wheat field, the contribution of stems to photosynthesis corresponds roughly to considering LAI* to be equal to $LAI + 1.5$ (A. Olioso, personal communication, 2000)). To roughly estimate the parameter b' , we considered that for the well-developed wheat field, $LAI^* \approx 6$ and vegetation water content $W_C \approx 2.6 \text{ kg/m}^2$ (from Figure 2), and parameter $b \approx 0.12$ from Wigneron *et al.* [1995]. Parameter b' can thus be roughly estimated from the simple formulation: $b' = \tau/LAI^* \approx (bW_C)/LAI^* \approx 0.05$. To investigate the sensitivity of the assimilation process to the value of b' , approach II was carried out for three values of b' surrounding the value $b' = 0.05$ ($b' = 0.03$, $b' = 0.05$, and $b' = 0.07$).

[21] The assimilation process in approach II was based on the coupled (ISBA-Ags/TB) model (Figure 4). In the ISBA-Ags model it is necessary to calibrate three main vegetation parameters that drive photosynthesis, senescence, and biomass allocation: leaf life expectancy (D_E), the ratio between metabolic biomass and leaf area index (B/LAI) and mesophyll conductance (g_M). Whereas g_M and D_E are genetic parameters of the plant, B/LAI is expected to vary according to the climatic conditions and nutrient availability. Therefore typical values of g_M and D_E may be obtained from previous studies based on field measurements and/or model

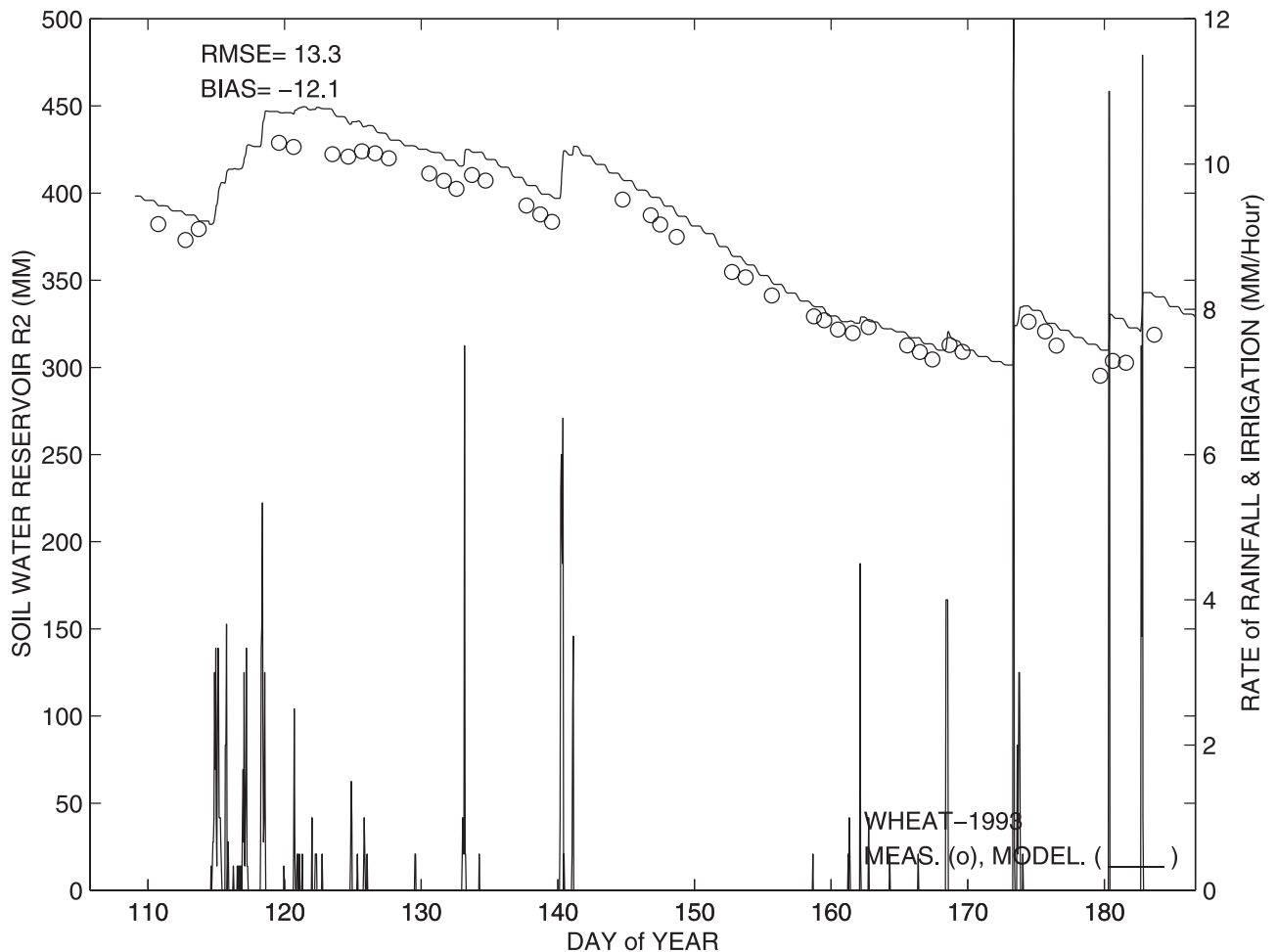


Figure 5. Time variations in soil water reservoir R_2 (mm) simulated by ISBA after calibration by the assimilation process (approach I). The simulations (solid lines) were compared with the observations (open circles). Rain and irrigation rates (mm h^{-1}) are indicated by vertical solid lines.

calibration, whereas B/LAI could be calibrated from remote sensing techniques.

[22] In this study, values of g_M and D_E ($g_M = 7 \text{ mm/s}$ and $D_E = 50 \text{ days}$) could be prescribed from average values obtained for C_3 crops in a previous study [Voirin, 1999]. In approach II, both the initial soil water reservoir R_2 at date $t = \text{DoY } 109$ ($R_{2-\text{INIT}}$) and the B/LAI ratio were retrieved from the assimilation process of the T_B data. The general principle of the assimilation process in approach II was the same as that for approach I: retrievals of both $R_{2-\text{INIT}}$ and B/LAI were carried out using a simple assimilation process consisting of minimizing the rms error between measured and simulated brightness temperatures during the DoY 109 to DoY 188 period. In this approach, B/LAI is a key parameter that drives both vegetation development (parameterized by both biomass and LAI^*) and vegetation optical thickness τ , through equation (4).

4. Results

4.1. Approach I

[23] In approach I, initial water content in the root zone ($R_{2-\text{INIT}}$) and time variations in optical depth τ were retrieved directly from the assimilation of the T_B measurements in the ISBA/TB model during an 80-day period (from

DoY 109 to DoY 188). Six parameters were retrieved: $R_{2-\text{INIT}}$ and the five parameters (K , a , T_I , b , T_S) describing time variations in τ using the parametric “growth curve” given by equation (1).

[24] The retrieval process consisted in minimizing the rms error between simulations and measurements of T_B (the obtained values were the following: rms error = 9.6K, bias = -0.5K for both polarizations and five incidence angles ($\theta = 0^\circ, 10^\circ, \dots, 40^\circ$)). Retrieved values from the assimilation approach were as follows: $R_{2-\text{INIT}} = 398.3 \text{ mm}$, $K = 0.506$, $a = 0.0814$, $T_I = 133.08$, $b = 0.074158$, $T_S = 165.96$. Using the retrieved value of $R_{2-\text{INIT}}$, ISBA simulations of $R_2(t)$ were carried out during the whole crop cycle and are illustrated in Figure 5. There was general close agreement between measured and simulated values of $R_2(t)$ (simulated data slightly overestimated measured values (rms error = 13.30 mm; mean bias = -12.1 mm)). Also, close agreement between measured and simulated surface variables was obtained from the SVAT simulations, in terms of surface soil moisture w_S and of energy and mass transfers (the rms error and mean bias between measured and simulated variables are given in Table 4).

[25] The retrieved time variations in τ were then compared to the measured vegetation variables. Usually, an

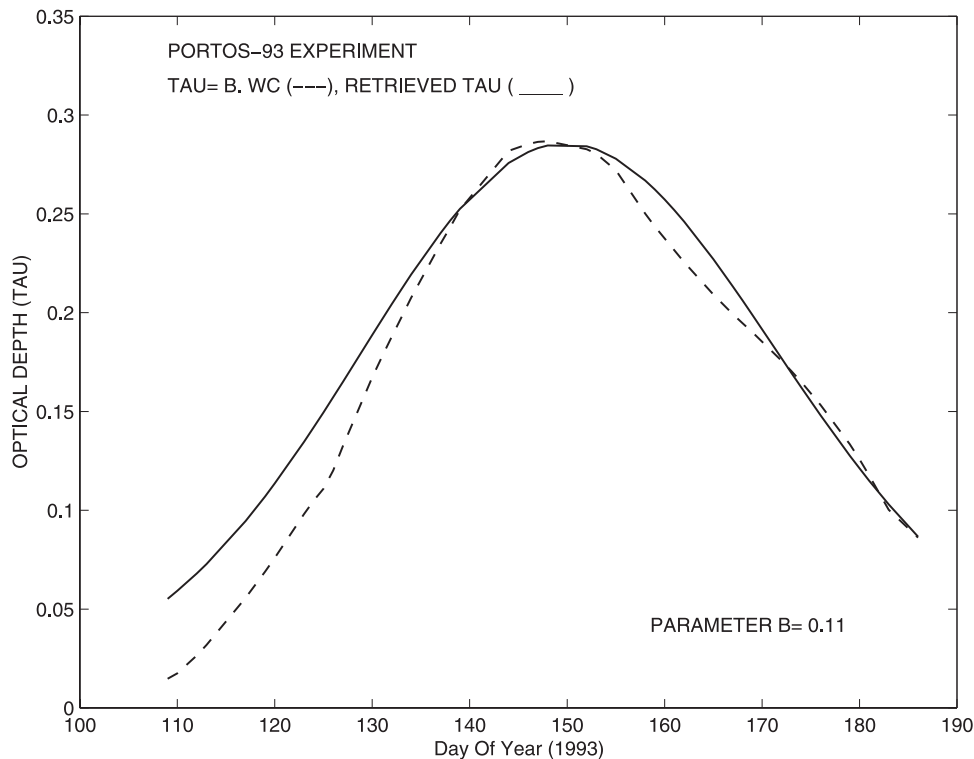


Figure 6. Comparison between retrieved (solid lines) and estimated (dashed lines) values of optical depth. Estimated values of optical depth (τ_W) were derived from ground measurements of the amount of water in the canopy W_C (kg/m^2) according to $\tau_W = b \cdot W_C$, where $b = 0.11$ (approach I).

estimate of optical depth (τ_W) can be obtained from ground-based measurements of vegetation water content W_C using equation (2). It is difficult to estimate a priori the value of b . A value of parameter $b = 0.15$ is considered to be representative of most agricultural crops, with the exception of grasses [Jackson and Schmugge, 1991]. Over the wheat field, Wigneron *et al.* [1995] found that the value of parameter b changed significantly during the crop cycle: b decreased from $b = 0.125$ for well-developed green vegetation down to $b = 0.04$ for a mature and senescent canopy. The time variations in retrieved τ were compared with τ_W , which was computed using equation (2) for different values of b ($b = 0.1, 0.11, 0.12, \dots, 0.15$). We found there was close correlation between both τ and τ_W , though the time variations in both terms were not strictly the same over the whole crop cycle. Closest agreement between τ and τ_W was obtained for $b = 0.11$ and the comparison between these two terms is shown in Figure 6.

4.2. Approach II

[26] In approach II, only two parameters were retrieved from the assimilation of the T_B measurements in the ISBA-Ags/TB model during the (DoY 109, DoY 188) period: the initial water content in the root zone ($R_{2\text{-INIT}} = R_2(t = \text{DoY } 109)$) and the parameter (B/LAI) which drives both vegetation development and time variations in vegetation optical thickness τ , from equation (4). As before, the retrieval process consisted in minimizing the rms error between simulations and measurements of T_B (for each value of b' , the rms error, averaged over both polar-

izations and five incidence angles ($\theta = 0^\circ, 10^\circ, \dots, 40^\circ$), was $\sim 10\text{--}11$ K). Using this approach, we retrieved values of both $R_{2\text{-INIT}}$ and B/LAI , for the three values of parameter b' (Table 3). Using these calibrated values, close agreement between measured and simulated surface variables was obtained from the ISBA-Ags simulations (the rms error and mean bias between measured and simulated variables are given in Table 4 for the three values of b'). It can be seen that though the range of possible values for b' we used in this study was wide (from 0.03 to 0.07), the results were generally quantitatively similar. Results were also similar to those obtained in approach I.

[27] Best results (both in terms of root zone soil moisture R_2 and evapotranspiration L_E) were obtained when b' was set at 0.07. For $b' = 0.03$ and $b' = 0.05$, it can be seen from Table 4 that the latent heat fluxes (L_E) were overestimated and slightly lower accuracy was obtained in the simulation of $R_2(t)$. To illustrate the results for $b' = 0.07$, a comparison between measured and simulated variables is given for R_2 in Figure 7, and for L_E and surface soil moisture (w_S) in Figures 8a and 8b. Also, simulations of T_B by the coupled ISBA-Ags/TB model simulations are illustrated in Figure 9

Table 3. Retrieved Values of Initial Root Zone Water Content $R_2(\text{DoY} = 109)$ and of Parameter B/LAI (Approach II)

	$b' = 0.03$	$b' = 0.05$	$b' = 0.07$
$R_2(\text{DoY} = 109)$, mm	421.7	406.5	382.05
B/LAI , kg/m^2	0.061	0.091	0.123

Table 4. Root-Mean-Square Error and Mean Bias Between Measured and Simulated Variables Over the Period (DoY 109 to DoY 188) for Both Approaches I and II^a

	Approach I	Approach II		
		$b' = 0.03$	$b' = 0.05$	$b' = 0.07$
Brightness temperature T_B , K (average for both polarizations and all angles)	9.6(-0.5)	10.2(2.5)	9.8(-2.5)	11.4(-4.6)
Soil water reservoir R_2 , mm	13.31(-12.1)	25.6(-14.6)	23.5(-17.0)	10.2(-7.1)
Surface soil moisture w_S [0-3 cm], m ³ /m ³	0.058(-0.01)	0.061(-0.031)	0.064(-0.028)	0.066(-0.011)
Evapotranspiration L_E (W/m ²) (DoY 109, DoY 165) period	36.0(0.0)	51.1(-18.9)	42.3(-8.8)	39.4(3.4)

^aThe measured minus simulated values are in parentheses.

at $\theta = 40^\circ$, when b' was set at 0.07 (as noted before, the rms error was $\sim 10-11$ K for each value of b'). The relatively high value of the rms error is mainly due to the inability of the simple TB model, used in this study, to account for the dependence of optical depth on polarization and angular effects (these effects are very large for vegetation canopies with a dominant vertical structure (stem dominated canopy) such as a wheat crop [Wigneron et al., 1995]). These effects can be seen in Figure 9, where the simulations cannot reproduce the large difference between H and V measured

brightness temperatures. Note that at satellite scales, very few studies have investigated the angular and polarization dependence of optical depth (τ). However, it is likely that this dependence is rather low, and specific problems due to the particular structure of the wheat canopy should not appear for space-borne observations over 30-50 km large pixels.

[28] In approach II the vegetation variables (LAI*, biomass, and optical depth) were obtained directly from the ISBA-Ags simulations. The simulations of LAI* for the

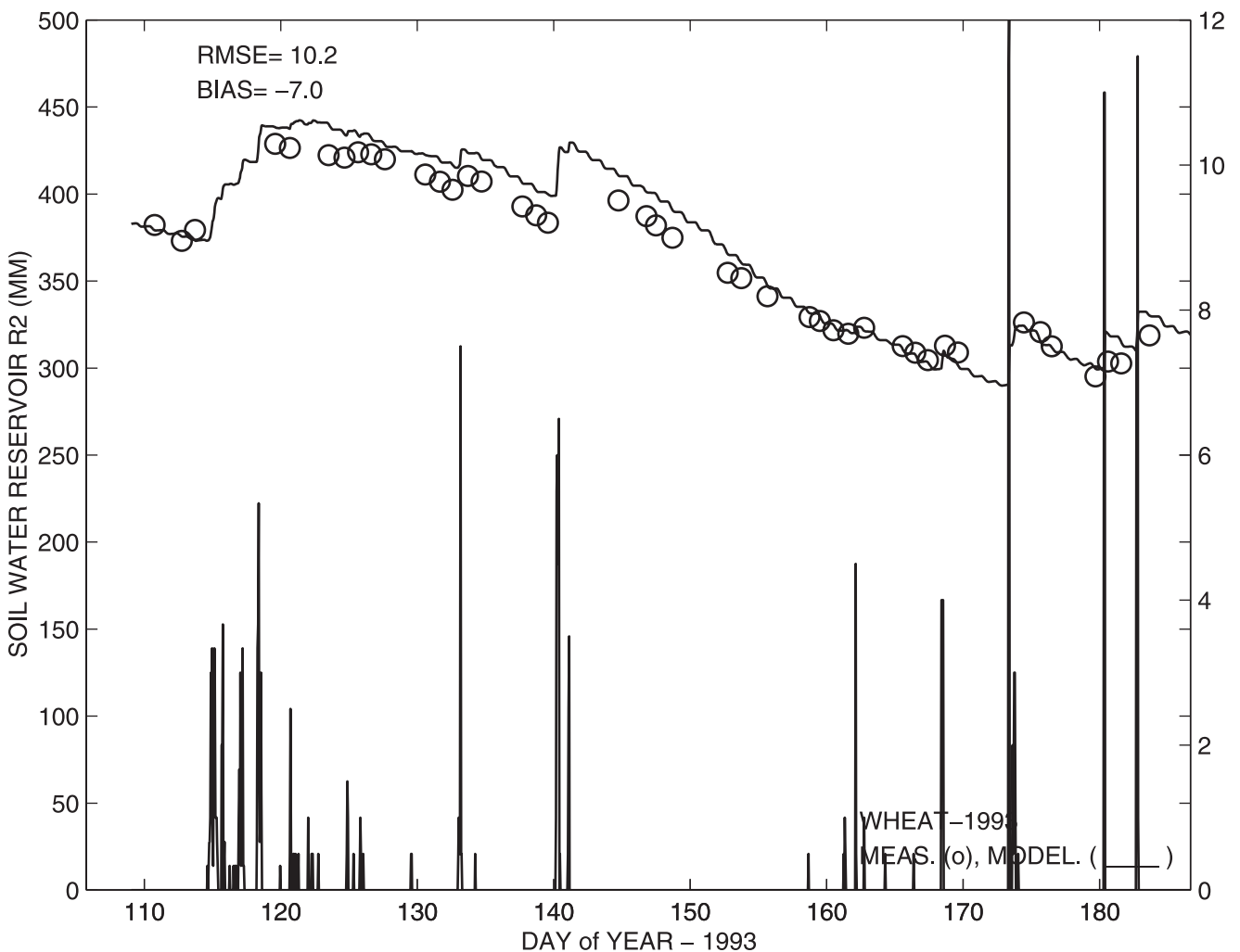


Figure 7. Time variations in soil water reservoir R_2 (mm) simulated by ISBA-Ags after calibration by the assimilation process (approach II). The simulations (solid line) were compared with the observations (open circles). Rain and irrigation rates (mm h⁻¹) are indicated by vertical solid lines.

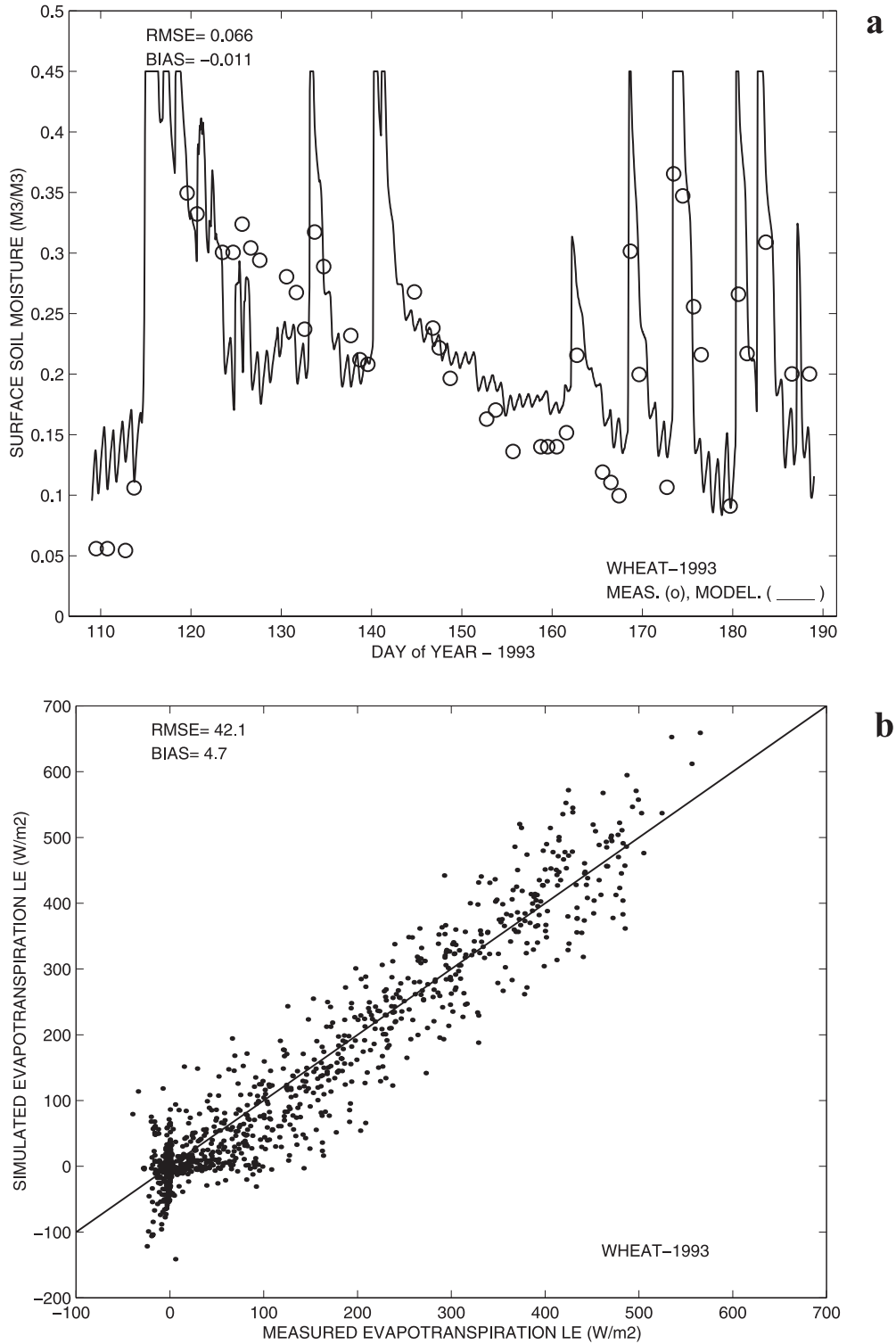


Figure 8. Comparison between measurements (open circles) and ISBA-Ags simulations (solid line) of (a) surface soil moisture (w_s) and (b) latent heat flux (L_E). The ISBA-Ags model was calibrated by the assimilation process (approach II).

three values of b' , are shown in Figure 10. As discussed in section 3.2, leaf area index LAI*, which is simulated by ISBA-Ags, is representative of the whole metabolic biomass that contributes to photosynthesis and plant transpiration.

An estimate of this term (referred to as plant area index (PAI)) was computed from the ground-based measurements as the sum of leaf area index and stem area index. Also, it was considered that the additive term (stem area index),

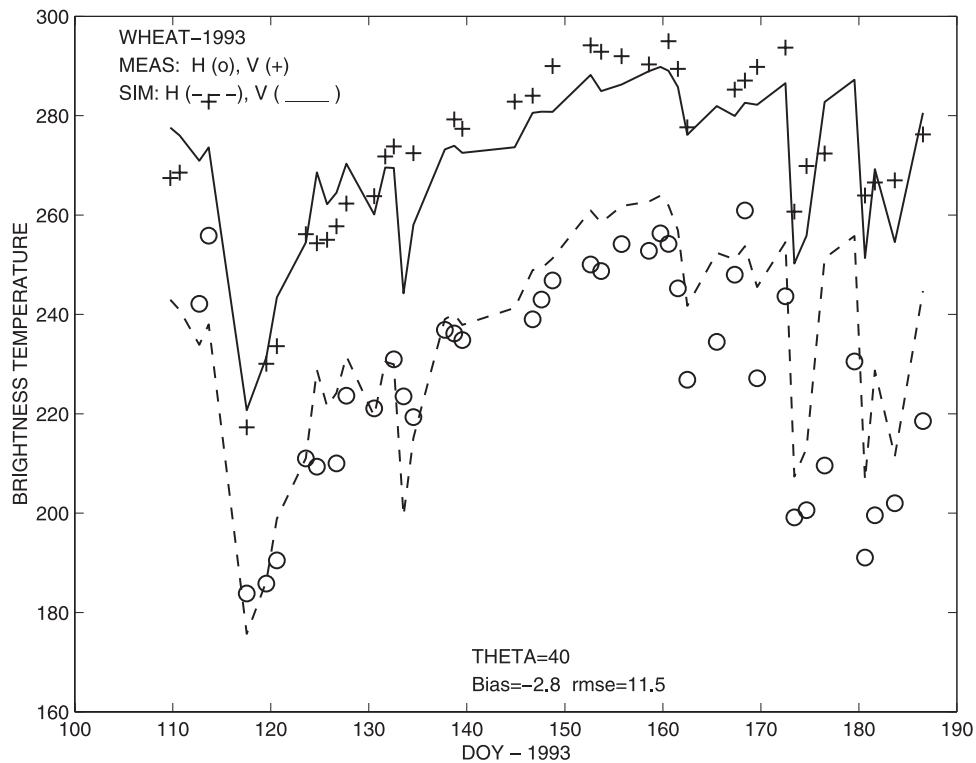


Figure 9. Comparison between measurements and simulations of brightness temperature T_B at $\theta = 40^\circ$ at both H and V polarizations by the coupled ISBA-Ags/TB model (approach II, using $b' = 0.07$).

which accounts for the contribution of stems to photosynthesis, did not exceed 1.5 for a well-developed canopy. The plant area index was thus computed as follows:

$$PAI = LAI + \text{stem area index} \quad (5a)$$

$$\text{stem area index} \leq 1.5 \quad (5b)$$

[29] Both the leaf area index (LAI) and the plant area index (PAI) are shown in Figure 10. It can be seen that the assimilation process can correctly detect and reproduce vegetation growth (the general trend of LAI* was very similar whatever the value selected for b'). The magnitude in the time variations of PAI and simulated LAI* (for $b' = 0.03$ and $b' = 0.05$) are very close. However, the maximum value of LAI* (LAI^*_{max}) was obtained on DoY 155, i.e., ~15 days later than the date of the maximum value for PAI (approximately on DoY 140). Note that the value of LAI^*_{max} appears to be almost linearly related to the value of b' .

5. Discussion and Conclusions

[30] Two main assimilation schemes of brightness temperature time series were tested in this study. The two approaches differed mainly with respect to how vegetation effects were accounted for, in terms of both vegetation biomass and vegetation optical depth. In approach I, on the basis of the coupled ISBA/TB model, LAI had to be prescribed using ancillary data (ground-based measurements in this study), and the optical depth was retrieved

directly from the assimilation approach. Approach II is a fully integrated approach that does not require ancillary data describing vegetation dynamics. In this approach, based on the coupled ISBA-Ags/TB model, both LAI and optical depth (by using equation (4)) are simulated, provided the coupled model is calibrated from the assimilation process.

[31] As discussed in the previous section, the data set we used was not large enough to carry out a quantitative comparison of both schemes. However, testing the implementation of the two assimilation approaches provided interesting information for a future possible operational use of the methods.

[32] The accuracy in the simulation of the surface variables (root zone and surface soil moisture, surface-atmosphere fluxes, surface temperature) was found to be very similar for both approaches. In approach II, retrievals of R_{2-INIT} were found to be slightly dependent on the value of parameter b' , relating the simulated LAI* to vegetation optical depth. Lower values of R_2 and of evapotranspiration fluxes (L_E) were obtained for higher values of b' . For a given value of measured brightness temperature (and thus of optical depth) the use of higher values of b' led to the simulation of lower LAI* values (since optical depth was computed as $\tau = b' \cdot LAI^*$). As LAI* is one of the main variables driving evaporation fluxes, lower LAI* values generally led to simulations of lower latent heat flux values (L_E). This effect also affected the retrieved values of root zone soil moisture R_{2-INIT} .

[33] In summary, both approaches I and II were found to be good candidates for the development of assimilation

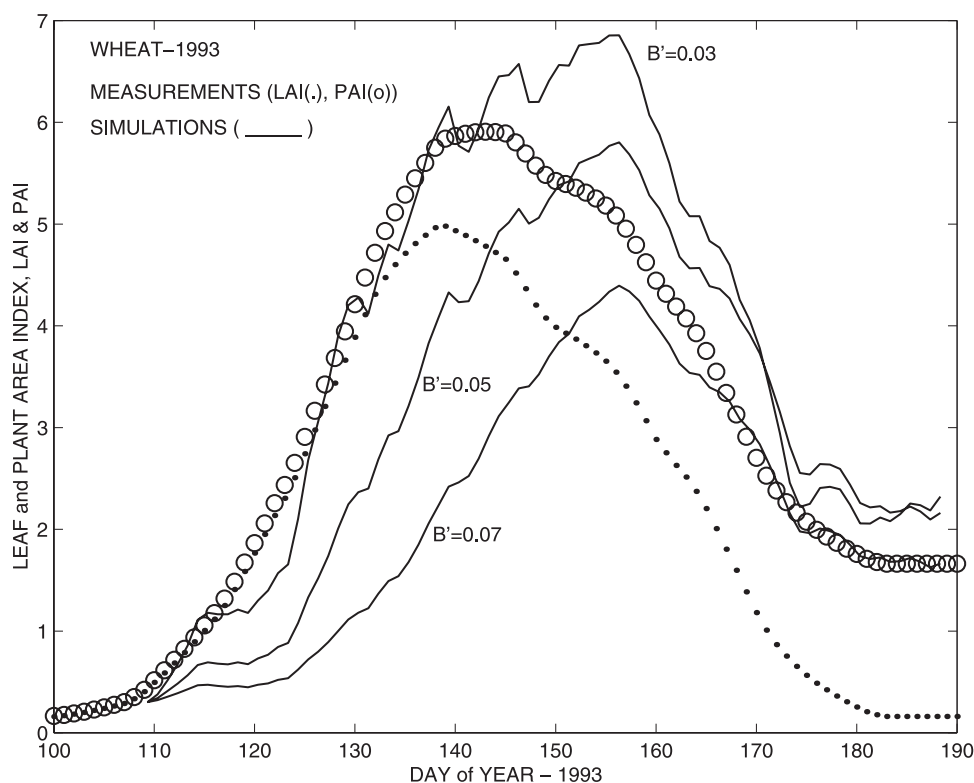


Figure 10. Comparison between ISBA-Ags simulations of LAI^* (solid line) for the three values of b' , and the ground-based measurements of green LAI (dotted line) and PAI (circled line) (approach II).

procedures of time series of passive microwave observations. For an operational use, the 80-day assimilation period, which was used in this work, may appear to be far too long. However, a few tests were carried out with shorter assimilation periods and good results were obtained. Emphasis in this study was placed on developing new modeling schemes and the tests that were carried out can provide a good basis for discussing the main principles of the proposed methods. Therefore no attempts were made in this work to optimize the duration of the assimilation process or to analyze the sensitivity of the results to the frequency of the T_B measurements involved in the retrieval process.

[34] Some limitations in the operational use of both approaches were revealed by this study:

1. In approach I, ancillary information is required to provide information on time variations in both leaf area index (LAI) and crop height (H_C). Both LAI and H_C are key variables in ISBA for simulating the fluxes at the soil-vegetation-atmosphere interfaces. This requirement cannot be met easily for practical applications on rather large spatial scales. Also, the functional form of vegetation dynamics is constrained by a “parametric growth curve” (given by equation (1)), which is mainly useful for crops. This constraint limits the possibility of monitoring a variety of conditions in vegetation development. For instance, this constraint may be too strong over natural areas in arid or semi-arid conditions, where vegetation growth can be very rapid and quite different from that of crops. However, for an operational use, the assimilation

period should be much shorter (less than 1 week). In this case and over rather large mixed SMOS pixels (~ 30 km at nadir), simple approaches could probably be implemented. For instance, the value of τ , assumed to be constant during a short period of time, could be retrieved concurrently with R_{2-INIT} from only several remote sensing observations.

2. Approach II is a fully integrated approach, in which optical depth can be derived from the ISBA-Ags simulations of leaf area index (LAI^*) using the multiplying factor b' . The sensitivity of the retrievals of R_{2-INIT} to the value of b' was found to be rather low.

[35] Owing to the assimilation scheme, the time variations in LAI^* were constrained to be closely related to time variations in optical depth (τ). Over the wheat field it was found that there was a general good agreement between the time variations in LAI^* and in the estimated plant area index (this variable is a ground-based estimate of the whole metabolic biomass contributing to photosynthesis). However, simulations of vegetation growth (namely leaf area index LAI^*) depend on the chosen value for b' . We already noted that there is no general relationship between LAI^* and optical depth τ over crops (equation (4) is an approximate relationship). Possibly the problem is different for large-scale space-borne observations. It is likely that simple and robust relationships between LAI^* and optical depth could be derived for each large-scale land cover type, before implementing the assimilation process. In that case assimilation results would be improved.

[36] Even though these basic limitations should be considered, very promising results were obtained from the two assimilation procedures described in this work. A key aspect of this study is that for both approaches, the results of the assimilation process confirmed the main results obtained from classical inversion approaches [Wigneron et al., 1995, 2000], e.g., the possibility to retrieve information on both soil and vegetation variables from dual-polarization and multiangular passive microwave observations. In classical inversion approaches, both soil moisture and optical depth could be retrieved, whereas the assimilation process allowed to retrieve information on the soil water reservoir R_2 (and vegetation optical depth), which is a key variable for estimating the evapotranspiration fluxes over land surfaces. It seems that the use of passive microwave data in the assimilation schemes could be self-consistent: no ancillary remote sensing observations were required to assimilate the brightness temperature data in this study. Also, very few calibration parameters are required for both the SVAT and TB models. Moreover, except for b' , it was possible to attribute the values of all these calibration parameters from the literature (these parameters are given in Tables 1 and 2). From the simple assimilation procedures of L band multiangular passive microwave observations proposed in this study, the coupled model SVAT/TB can be used to simulate all the key terms in the mass and energy fluxes at the soil-vegetation-atmosphere interfaces: root zone and surface soil moisture, surface-atmosphere fluxes, surface temperature, etc. These results demonstrate the large potential of L band multiangular microwave radiometric observations for monitoring both soil and vegetation characteristics. Thus promising assimilation schemes can be expected from the SMOS L band sensor (with dual-polarization and multiangular capabilities) over land surface in the fields of meteorology and hydrology.

[37] **Acknowledgments.** The authors wish to thank to Joël Noilhan (Météo-France, Toulouse), Frédéric Huard (INRA AGROCLIM, Avignon) for helpful conversations and suggestions concerning this paper. We are grateful to Anne-Marie Wall for revising the english version of the manuscript (INRA Translation Unit, Jouy-en-Josas).

References

- Burke, E. J., R. J. Gurney, L. Simmonds, and T. J. Jackson, Calibrating a soil water and energy budget model with remotely sensed data to obtain quantitative information about the soil, *Water Resour. Res.*, **33**, 1689–1697, 1997.
- Calvet, J.-C., J. Noilhan, and P. Bessemoulin, Retrieving the root-zone soil moisture from surface soil moisture or temperature estimates: A feasibility study based on field measurements, *J. Appl. Meteorol.*, **37**(4), 371–386, 1998a.
- Calvet, J.-C., J. Noilhan, J.-L. Roujean, P. Bessemoulin, M. Cabelguenne, A. Olioso, and J.-P. Wigneron, An interactive vegetation SVAT model tested against data from six contrasting sites, *Agric. For. Meteorol.*, **92**, 73–95, 1998b.
- Calvet, J.-C., et al., MUREX: A land-surface field experiment to study the annual cycle of the energy and water budgets, *Ann. Geophys.*, **17**, 838–854, 1999.
- Calvet, J.-C., J. Noilhan, and J.-P. Wigneron, Root-zone soil moisture analysis using microwave radiometry, paper presented at 8th Symposium on Physical Measurements and Signatures in Remote Sensing, Int. Soc. for Photogramm. and Remote Sens., Aussois, France, 2001.
- Chanzy, A., and L. Bruckler, Significance of soil surface moisture with respect to daily bare soil evaporation, *Water Resour. Res.*, **29**, 1113–1125, 1993.
- Daamen, C. C., and L. P. Simmonds, Measurement of evaporation from bare soil and its estimation using surface resistance, *Water Resour. Res.*, **32**, 1393–1402, 1996.
- Entekhabi, D., H. Nakamura, and E. G. Njoku, Solving the inverse problem for soil moisture and temperature profiles by sequential assimilation of multifrequency remotely sensed observations, *IEEE Trans. Geosci. Remote Sens.*, **32**, 438–447, 1994.
- Galantowicz, J. F., D. Entekhabi, and E. G. Njoku, Tests of sequential data assimilation for retrieving profile soil moisture and temperature from observed L -band radiobrightness, *IEEE Trans. Geosci. Remote Sens.*, **37**, 1860–1870, 1999.
- Habets, F., Modélisation du cycle continental de l'eau à l'échelle régionale. Application aux bassins de l'Adour et du Rhône, doctoral thesis, Univ. of Toulouse III, Toulouse, France, 6 March 1998.
- Jackson, T. J., and T. J. Schmugge, Vegetation effects on the microwave emission of soils, *Remote Sens. Environ.*, **36**, 203–212, 1991.
- Jackson, T. J., D. M. Le Vine, A. Y. Hsu, A. Oldak, P. J. Starks, C. T. Swift, J. D. Isham, and M. Haken, Soil moisture mapping at regional scales using microwave radiometry: The Southern Great Plains Hydrology Experiment, *IEEE Trans. Geosci. Remote Sens.*, **37**, 2136–2150, 1999.
- Jacobs, C. M. J., B. J. van den Hurk, and H. A. R. de Bruin, Stomatal behaviour and photosynthetic rate of unstressed grapevines in semi-arid conditions, *Agric. For. Meteorol.*, **80**, 111–134, 1994.
- Kerr, Y., et al., MIRAS on RAMSES: radiometry applied to soil moisture and salinity measurements, Full Proposal to the AO Earth Explorer Opportunity Missions, Eur. Space Agency, Paris, 31 Nov. 1999.
- Njoku, E. G., and D. Entekhabi, Passive microwave remote sensing of soil moisture, *J. Hydrol.*, **184**, 101–129, 1996.
- Noilhan, J., and J. C. Calvet, Mesoscale land-atmosphere models and data needs, in *Passive Microwave Remote Sensing of Land-Atmosphere Interactions*, ESA/NASA Int. Workshop 1993, pp. 17–54, edited by B. J. Choudhury et al., VSP, Utrecht, Netherlands, 1995.
- Noilhan, J., and S. Planton, A simple parameterization of land surface processes for meteorological models, *Mon. Weather Rev.*, **117**, 536–549, 1989.
- Raju, S., A. Chanzy, J.-P. Wigneron, J.-C. Calvet, Y. Kerr, and L. Laguerre, Soil moisture and temperature profile effects on microwave emission at low frequencies, *Remote Sens. Environ.*, **54**, 85–97, 1995.
- Reichle, R. H., D. Entekhabi, and D. B. McLaughlin, Downscaling of Radiobrightness measurements for soil moisture estimation: A four-dimensional variational data assimilation approach, *Water Resour. Res.*, **37**, 2353–2364, 2001.
- Schmugge, T. J., and T. J. Jackson, Mapping soil moisture with microwave radiometers, *Meteorol. Atmos. Phys.*, **54**, 213–223, 1994.
- Schmugge, T. J., P. Gloersen, T. T. Wilheit, and F. Geiger, Remote sensing of soil moisture with microwave radiometers, *J. Geophys. Res.*, **79**, 317–323, 1974.
- Ulaby, F. T., R. K. Moore, and A. K. Fung, *Microwave Remote Sensing: Active and Passive*, vol. 3, Artech House, Norwood, Mass., 1986.
- Voirin, S., Application du schéma de surface ISAB-Ags au bassin versant de l'Adour: étalonnage et simulation des bilans hydriques et énergétiques, International Report of Météo-France, Toulouse, France, 1999.
- Wigneron, J.-P., A. Chanzy, J.-C. Calvet, and N. Bruguier, A simple algorithm to retrieve soil moisture and vegetation biomass using passive microwave measurements over crop fields, *Remote Sens. Environ.*, **51**, 331–341, 1995.
- Wigneron, J.-P., J.-C. Calvet, and Y. Kerr, Monitoring water interception by crop fields from passive microwave observations, *Agric. For. Meteorol.*, **80**, 177–194, 1996.
- Wigneron, J.-P., A. Olioso, J.-C. Calvet, and P. Bertuzzi, Estimating root-zone soil moisture from surface soil moisture data and SVAT modeling, *Water Resour. Res.*, **35**, 3735–3745, 1999a.
- Wigneron, J.-P., P. Ferrazzoli, A. Olioso, P. Bertuzzi, and A. Chanzy, A simple approach to monitor crop biomass from C-band radar data, *Remote Sens. Environ.*, **60**, 179–188, 1999b.
- Wigneron, J.-P., P. Waldteufel, A. Chanzy, J.-C. Calvet, and Y. Kerr, Two-D microwave interferometer retrieval capabilities of over land surfaces (SMOS Mission), *Remote Sens. Environ.*, **73**, 270–282, 2000.

J.-C. Calvet, Météo France/Centre National de Recherche de la Météorologie, 42 Avenue G. Coriolis, 31057 Toulouse, Cedex 1, France.
 A. Chanzy and A. Olioso, Institut National de la Recherche Agronomique, Climat, Sol et Environnement, Agroparc, 84914 Avignon Cedex 9, France.
 Y. Kerr, Centre National d'Etudes Spatiales/Centre d'Etude Spatial de la Biosphère, 18 Avenue Ed. Belin, 31401 Toulouse Cedex 4, France.
 J.-P. Wigneron, Institut National de la Recherche Agronomique, Unité de Bioclimatologie, B.P. 81, 33883 Villenave d'Ormon Cedex, France. (wigneron@bordeaux.inra.fr)